5th Workshop on Galactic Chemodynamics

CSIRO PUBLISHING

Publications of the Astronomical Society of Australia, 2004, **21**, 216–221 www.publish.csiro.au/journals/pasa

Interactions of Satellite Galaxies in Cosmological Dark Matter Halos

Alexander Knebe[1,2]*, Stuart P. D. Gill*[1]*, and Brad K. Gibson*[1]

[1] Centre for Astrophysics & Supercomputing, Swinburne University, Hawthorn VIC 3122, Australia
[2] E-mail: aknebe@astro.swin.edu.au

Received 2004 February 16, accepted 2004 March 16

Abstract: We present a statistical analysis of the interactions between satellite galaxies in cosmological dark matter halos taken from fully self-consistent high-resolution simulations of galaxy clusters. We show that the number distribution of satellite encounters has a tail that extends to as many as three to four encounters per orbit. On average 30% of the substructure population had at least one encounter (per orbit) with another satellite galaxy. However, this result depends on the age of the dark matter host halo with a clear trend for more interactions in younger systems. We also report a correlation between the number of encounters and the distance of the satellites to the centre of the cluster — satellite galaxies closer to the centre experience more interactions. However, this can be simply explained by the radial distribution of the substructure population and merely reflects the fact that the density of satellites is higher in those regions.

In order to find substructure galaxies we applied (and present) a new technique based upon the N-body code MLAPM. This new halo finder MHF (MLAPM's halo finder) acts with exactly the same accuracy as the N-body code itself and is therefore free of any bias and spurious mismatch between simulation data and halo finding precision related to numerical effects.

Keywords: methods: N-body simulations — galaxies: clusters — galaxies: kinematics and dynamics — cosmology: dark matter

1 Introduction

1.1 Observations

There are several hints indicating that satellite galaxies orbiting within our own Milky Way are interacting with each other. Zhao (1998), for instance, proposed a scenario where the Sagittarius Dwarf galaxy had an encounter with the Magellanic Cloud system some 2–3 Gyr ago, something that has also been speculated and noted by Ibata & Lewis (1998). Moreover, the two Magellanic Clouds themselves are another example of an interacting pair of substructure galaxies. It has also been noted by Moore et al. (1996) that 'galaxy harrasment' in cosmological simulations of galaxy cluster evolution will lead to a morphology change of satellite galaxies.

However, the literature to date lacks a statistical analysis of interacting satellite galaxies orbiting within the potential of a common dark matter host halo. How frequent are satellite–satellite encounters and where in the galaxy cluster do they happen? Furthermore, observations of the Local Group Dwarfs indicate a clear correlation between star formation activity and the distance of the respective Dwarf to the centre of the Milky Way (van den Bergh 1994) with satellites farther away showing stronger activity. Can this be ascribed to satellite–satellite interactions? The aim of this study is to quantify such interactions in galaxy clusters derived from fully self-consistent cosmological N-body simulations within the framework of the currently accepted Cold Dark Matter (CDM) structure formation scenario.

1.2 Is Cold Dark Matter Still Feasible?

There is mounting, if not overwhelming, evidence that CDM provides the most accurate description of our Universe. Observations point towards a ΛCDM Universe comprised of 28% dark matter, 68% dark energy, and luminous baryonic matter (i.e. galaxies, stars, gas, and dust) at a mere 4% (compare Spergel et al. 2003). This 'concordance model' induces hierarchical structure formation whereby small objects form first and subsequently merge to form progressively larger objects (e.g. White & Rees 1978; Davis et al. 1985). Hence, galaxies and galaxy clusters are constantly fed by an accretion stream of smaller entities starting to orbit within the encompassing dark matter potential of the host. While generally successful, the ΛCDM model does face several problems, one such problem actually being the prediction that one-to-two orders of magnitude more satellite galaxies should be orbiting within galactic halos than are actually observed (Klypin et al. 1999; Moore et al. 1999).

However, there are also indications that the CDM model is in fact correct and does *not* have a problem with an overabundant population of satellite galaxies. For instance, Benson et al. (2002) carried out a semi-analytical study of satellites in the Local Group and found that an

 10.1071/AS04018 1323-3580/04/02216

earlier epoch of reionisation was sufficient to suppress star formation in many of the subhalos and thus produce a significant population of 'dark galaxies'.

Therefore, if the CDM model is in fact correct and the (overabundant) population of (dark) satellites predicted by it really does exist, it is imperative to understand the discrepancy by investigating the orbital evolution of these objects and their deviation from the background dark matter distribution.

1.3 The Story, So Far

To date, typical satellite properties such as orbital parameters and mass loss under the influence of the host halo have primarily been investigated using *static* potentials for the dark matter host halo (Johnston et al. 1996; Hayashi et al. 2003). We stress that each of these studies has provided invaluable insights into the physical processes involved in satellite disruption; our goal is to augment those studies by relaxing the assumption of a static host potential as, in practice, realistic dark matter halos are neither static nor spherically symmetric.

1.4 The Story Continues

The work presented here is based upon a set of numerical simulations of structure formation within the said concordance model, analysing in detail the temporal and spatial properties of satellite galaxies residing within host dark matter halos that formed fully self-consistently within a cosmological framework. We focus on interactions between satellite galaxies orbiting within a larger dark matter halo and especially if there is a relation between mutual interplay and distance to the host. The outline of the paper is as follows. In Section 2 we present our new halo finding algorithms based upon the N-body code `MLAPM`. We then apply it to our set of eight cosmological dark matter halos in Section 3 with a summary of our results given in Section 4.

2 Identifying Satellite Galaxies

2.1 Cosmological Simulations

Over the last decades great advancements have been made in the development of N-body codes. We have seen the rise of tree-based gravity solvers (Barnes & Hut 1986), mesh-based techniques (Klypin & Shandarin 1983), and combinations of direction summation techniques and grid-based Poisson solvers (Efstathiou et al. 1985). However, simulating the Universe in a computer and producing the data is only the first step in a long journey; the purpose of these codes is their predictive power, thus the ensembles of millions of dark matter particles used with such (dissipationless) N-body codes need to be interpreted and then compared to the observable Universe. This task requires analysis tools to map the phase space, which is being sampled by the particles, back to 'real' objects in the Universe, the traditional way has been through the use of 'halo finders'.

2.2 Identifying Dark Matter Halos

Halo finders mine the N-body data to find locally overdense gravitationally bound systems. Under the assumption that all galaxies and galaxies clusters are centred about local over-density peaks in the dark matter density field they are usually found just using spatial information of the particle distribution. To identify objects in this fashion, the halo finder is required in some way to reproduce the work of the N-body solver in the calculation of the density field and the location of its peaks. The major limitation, however, will always be the appropriate reconstruction of the density field. Normally this task is performed *after* the simulation has finished using an independent method to derive (1) the density field and (2) to smooth it on a certain scale. With that in mind, we are using a new method for identifying gravitationally bound objects that utilises the adaptive meshes of the open source N-body code `MLAPM`[1] (Knebe, Green, & Binney 2001). It is called `MHF` (`MLAPM`'s Halo Finder) and naturally works on-the-fly, but has also been adapted to deal with single outputs of any N-body code. However, in order to understand the functionality of `MHF` it is important to gain insight into the mode of operation of `MLAPM` first.

2.3 `MLAPM`'s Mode of Operation

`MLAPM` reaches high force resolution by refining high-density regions with an automated refinement algorithm. These adaptive meshes are recursive — refined regions can also be refined, each subsequent refinement having cells that are half the size of the cells in the previous level. This creates a hierarchy of refinement meshes of different resolutions covering regions of interest. The refinement is done cell by cell (individual cells can be refined or de-refined) and meshes are not restricted to have a particular symmetry. The criterion for (de-)refining a cell is simply the number of particles within that cell and a detailed study of the appropriate choice for this number can be found elsewhere (Knebe et al. 2001). `MLAPM`'s adaptive refinement meshes therefore follow the density distribution by construction. Thus, the grid structure naturally surrounds the (satellite) galaxies as they manifest themselves as overdensities in the underlying background field, an example of which can be viewed in Figure 1 where we show a slice through a sample ΛCDM simulation. In the left panels the actual particle distribution is presented whereas the right panels indicate the adaptive meshes invoked by `MLAPM` to solve Poisson's equation and integrate the equations of motion, respectively. In the lower right panel the white circle highlights the ability of `MLAPM`'s grid to locate substructure — only on the finest refinement level does

[1] `MLAPM` can be downloaded from `http://astronomy.swin.edu.au/MLAPM`

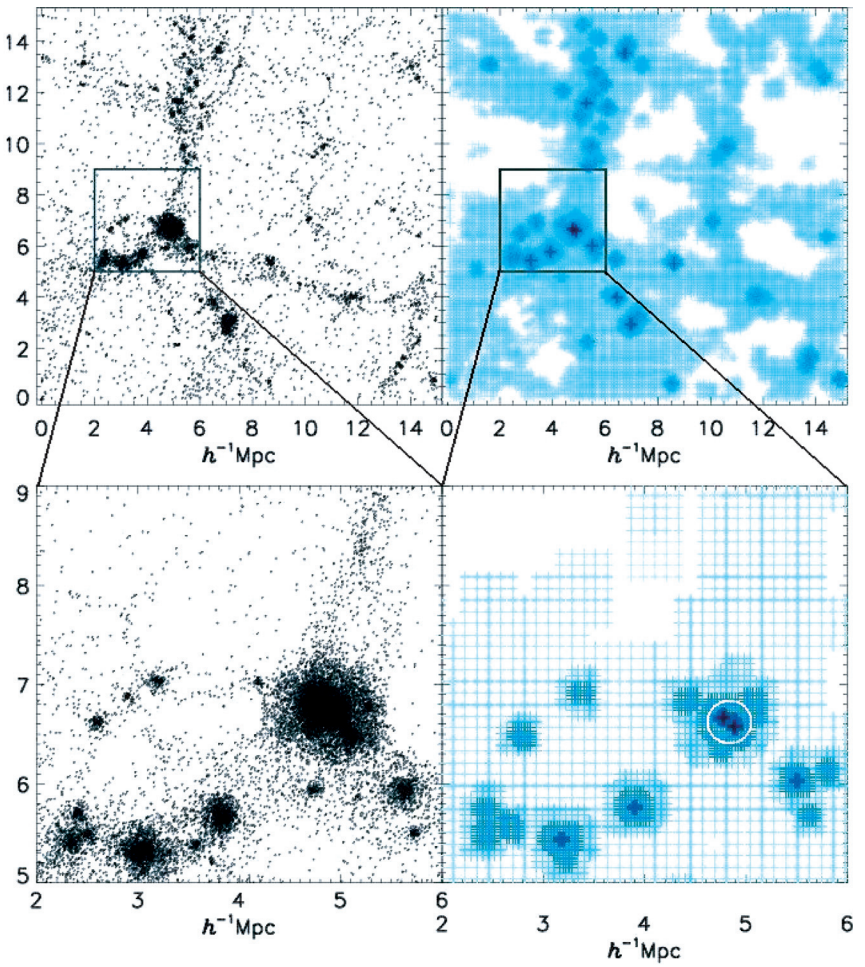

Figure 1 MLAPM at work. The upper panels show a sample cosmological ΛCDM simulation with the lower panels a magnification of the marked region. In the left panels the particle positions are plotted whereas the right panels are indicating the (adaptive) grid points used to solve the governing equations of motion. The circle in the lower right panel highlights substructure being picked up by the finest refinement grid.

it become apparent that the massive galaxy cluster in fact has two centres, which is a mere reflection of the fact it recently underwent a major merger with the two progenitors still not fully coalesced yet. The advantage of reconstructing and using these adaptive grids to identify prospective halo centres is that they naturally follow the density field with the *exact* accuracy of the N-body code.

2.4 MHF (MLAPM's Halo Finder)

In Figure 1 we have seen the capability of MLAPM to localise local overdensity peaks in cosmological simulations of structure formation. But this is just the first step to identifying gravitationally bound objects. To actually locate dark matter halos within the simulation data we build a register of positions of the peaks in the density field from the full adaptive grid structure invoked by MLAPM using the same refinement criterion as for the original runs; we build a list of 'potential centres'. To do this we restructure the hierarchy of nested, isolated MLAPM grids into a 'grid tree', storing the centre of the densest grid in the end of each branch. For each of these potential centres we step out in radial bins until the overdensity (measured in terms of the cosmological background density) drops below the virial value set by the background cosmological model, i.e. $\Delta_{\rm vir} = 340$ for ΛCDM at redshift $z = 0$. This defines the virial radius $R_{\rm vir}$ and provides us with a list of particles associated with that dark matter halo.

We then need to prune that list and remove (in an iterative procedure) all gravitationally unbound particles. Starting with the potential centre again, we calculate the kinetic and potential energy for each individual particle in the respective reference frame, and all particles faster than twice the escape velocity are removed from the halo. We then recalculate the centre (as well as the virial radius) and proceed through the process again. This iteration stops once no further particles are removed or if there are fewer than eight particles left, in which case the potential centre will be removed from the halo list completely.

In the end we are left with not only a list of appropriate halo positions but we also derived canonical properties for all credible objects, such as virial radius, virial mass, velocity dispersion, and density profile. A more elaborate description of our technique can be found elsewhere though (Gill, Knebe, & Gibson 2004a).

3 Quantifying Interactions in Simulated Galaxy Clusters

3.1 The Dark Matter Host Halos

We created a set of eight high-resolution galaxy clusters each consisting of order more than a million dark matter particles. These clusters formed in dissipationless N-body simulations of the 'concordance' (ΛCDM) cosmology ($\Omega_0 = 0.3$, $\Omega_\lambda = 0.7$, $\Omega_b h^2 = 0.022$, $h = 0.7$, $\sigma_8 = 0.9$). The runs have a mass resolution of $m_p = 1.6 \times 10^8 h^{-1}\,\mathrm{M}_\odot$ and achieved a force resolution of approximately $2h^{-1}$ kpc allowing us to resolve the host halos down to about the central 0.25% of their virial radii $R_{\rm vir}$.

The halos were specifically selected to investigate the evolution of satellite galaxies and its debris in an unbiased sample of host halos thus analysing the influence of environment in the evolution of such systems. To achieve this goal, high-quality temporal information was required to track the development of the satellites. We therefore stored 17 outputs from $z = 2.5$ to $z = 0.5$ equally spaced with $\Delta t \approx 0.35$ Gyr. From $z = 0.5$ to $z = 0$ we have 30 outputs spaced $\Delta t \approx 0.17$ Gyr. A summary of the eight host halos is presented in Table 1.

The quality of our halo finder and our data, respectively, can be viewed in Figure 2. There we show the orbits of four sample satellite galaxies orbiting within their respective host halo. This Figure nicely demonstrates how we are very accurately tracking the orbits of the satellites within the area of trade of the host halos. In a companion paper (Gill et al. 2004c) we present a thorough analysis of the dynamics of these satellite galaxies. There we also present the number distribution of orbits of the substructure population which peaks at about one to two orbits with a tail extending to as many as five orbits in the older systems. However, in this study we like to focus on one particular aspect, namely satellite–satellite encounters.

3.2 Quantifying Encounters

As a first order approximation for quantifying encounters between substructure galaxies we calculated the tidal radius of a given satellite *induced by one of the other satellites*. This means that the tidal radius is defined to be the radius where the gravitational effects of the companion satellite are greater than its self-gravity. When approximating both satellites as point masses and maintaining that the mean density within the satellite has to be three times the mean density of the 'perturber' at distance D (Jacobi limit) the definition for tidal radius reads as follows

$$r_{\rm tidal} = \left(\frac{m}{3M}\right)^{1/3} D, \qquad (1)$$

where m is the mass of the actual satellite and M is the mass of the perturbing satellite at distance D.

Whenever the tidal radius becomes smaller than the virial radius[2] of the satellite we increased a counter for that particular satellite. This counter now keeps track of the number of (perturbing) interactions with companion satellite galaxies. As some of the satellites may have had more interactions simply because they spent more time orbiting the host, we are normalising the number of encounters by the number of orbits for each individual satellite. The distribution of this (normalised) counter is presented in Figure 3. The pronounced peak at zero encounters shows that in most cases the interactions between satellites is negligible. However, we also observe that (in our simplistic treatment for satellite–satellite interactions) we do find as many as three to four encounters per orbit for individual satellites. This, in fact, indicates that with sufficient (spatial) resolution (as it is the case with our data) one is able

[2] We are tracking each satellite galaxy individually from the formation time of the host halo using its initial particle content and hence we are in the unique position to accurately calculate its virial radius as the radius where the mean averaged density (measured in terms of the cosmological background density ρ_b) drops below $\Delta_{\rm vir}(z)$.

Table 1. Properties of the eight dark matter host halos. Distances are measured in h^{-1} Mpc, velocities in km s^{-1}, masses in $10^{14}h^{-1}\,\mathrm{M}_\odot$, and the age in Gyr

We applied a mass-cut of $M > 10^{10}h^{-1}\,\mathrm{M}_\odot$ (100 particles) which explains the rather 'low' number for $N_{\rm sat}(<R_{\rm vir})$

Halo	$R_{\rm vir}$	$M_{\rm vir}$	$z_{\rm form}$	Age	$N_{\rm sat}(<R_{\rm vir})$
#1	1.34	2.87	1.16	8.30	158
#2	1.06	1.42	0.96	7.55	63
#3	1.08	1.48	0.87	7.16	87
#4	0.98	1.10	0.85	7.07	57
#5	1.35	2.91	0.65	6.01	175
#6	1.05	1.37	0.65	6.01	85
#7	1.01	1.21	0.43	4.52	59
#8	1.38	3.08	0.30	3.42	251

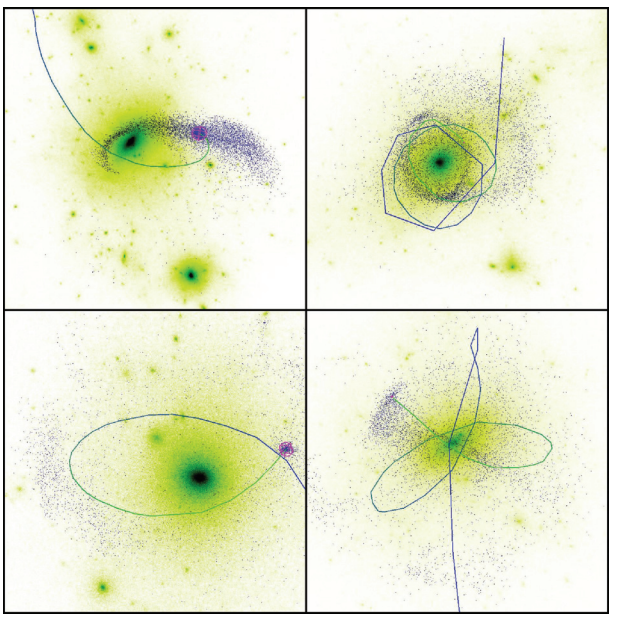

Figure 2 Some sample orbits of satellite galaxies within our set of dark matter host halos. We can clearly see how well we trace the orbits and follow the tidal disruption of the satellites, respectively.

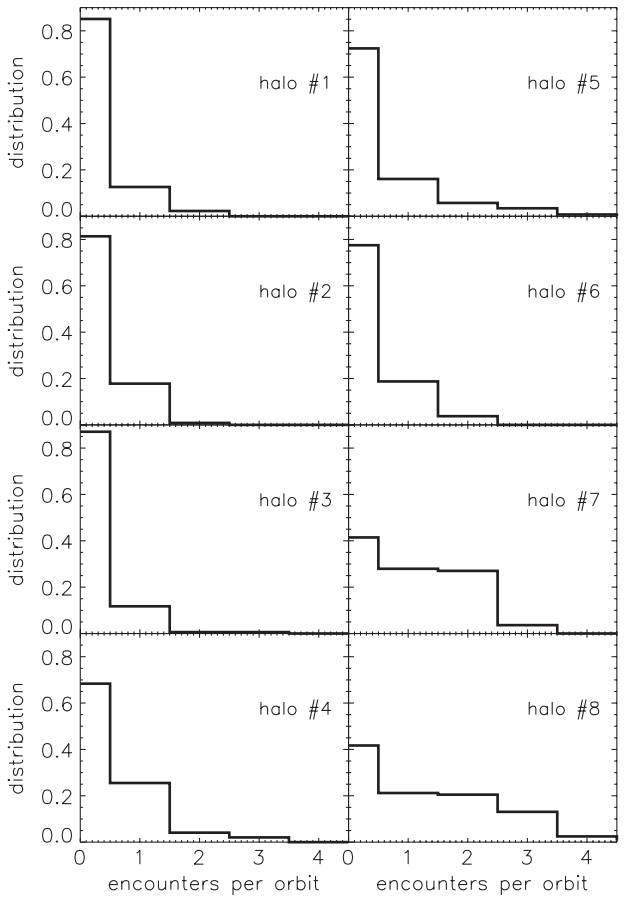

Figure 3 Distribution of number of encounters for all satellite galaxies more massive than $10^{10}h^{-1}\,M_{\odot}$ at redshift $z=0$.

Table 2. Percentage of satellites that had one or more encounters per orbit

Halo	Percentage
#1	14
#2	18
#3	12
#4	31
#5	27
#6	22
#7	58
#8	58

to decipher the influence of the dominant host halo from the (more minor) interactions with the companion satellite galaxies. We, however, leave a detailed analysis of this phenomenon to a companion paper (Knebe et al. 2004), where we individually select satellite galaxies and resimulate them in static and evolving analytic host potentials as opposed to their evolution in the live potential used for this study.

We complement Figure 3 with Table 2 where we give the percentage of satellites that had one or more encounters per orbit. The average percentage amounts to 30% of the whole substructure population. We also observe a clear trend for the interactions to become more prominent in younger systems. This is basically a reflection of the

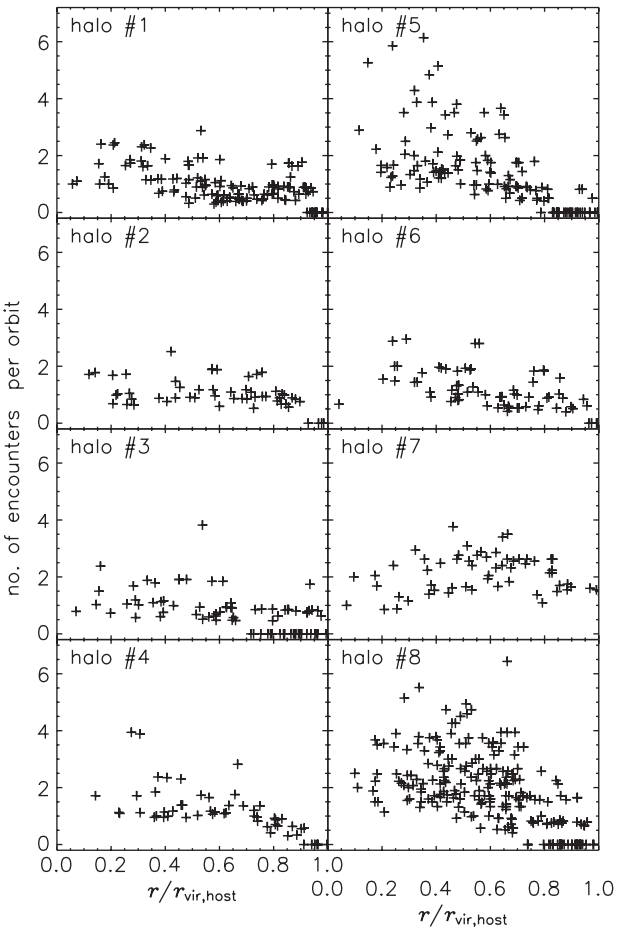

Figure 4 Encounters per orbit as a function of distance to the host halo's centre for redshift $z=0$.

fact that the younger systems are still in the process of digesting their last major merger and have not yet reached an equilibrium state.

3.3 Relation to Observations

If we now assume that such interactions might be held responsible for star formation bursts, that is, if encounters trigger star formation, it raises the question whether we can explain the observed correlation between star formation activity in the Local Group Dwarfs and distance to the centre of the Milky Way. Van den Bergh (1994), for instance, reported that Dwarf spheroidals located close to the Galaxy only experienced star formation early in their lifetimes. Dwarf spheroidals at intermediate distances underwent significant star formation more recently whereas the most distant ones do show ongoing star formation at the present time. Do encounters with other satellites trigger star formation bursts? To this extent we present the relation between the number of encounters (per orbit) as a function of distance to the centre of the host at redshift $z=0$. The result can be viewed in Figure 4. Unfortunately we do not observe a clear trend for all our halos, even though most of them actually show the reverse correlation — the closer a satellite passes to the centre of the host galaxy, the greater the number of encounters

with the other substructure. This relation is even more prominent when not normalising by the number of orbits. Only halo #7 shows a trend that agrees with the observational finding for star formation activity and distance to the centre, even though we show in Gill et al. (2004) that halo #7 does otherwise have no outstanding differences to the other halos. Anyway, as we see in Gill, Knebe, & Gibson (2004a) the radial satellite density distribution roughly declines like $\rho_{\rm sat} \propto r^{-2}$ and hence the mild (anti-) correlation between number of encounters and distance can be interpreted as a 'volume effect' — closer to the centre of the host are found approximately the same number of satellites in a spherical shell as farther out, but as the volume of that shell is smaller the satellites are more likely to interact.

4 Summary

We used a set of eight high-resolution cosmological simulations to investigate and quantify interactions between satellite galaxies orbiting within a common dark matter halo. Using our definition for encounter, which is based upon the mutually induced tidal radius, we showed that on average 30% of the substructure population had had more than one encounter per orbit with another satellite galaxy orbiting within the same host halo. There is, however, a clear trend for interactions to be more common in young galaxy clusters. We furthermore showed that satellite galaxies closer to the centre of the host halo had had more interactions with companion satellites, not because they simply orbited for longer in the underlying host potential but most likely because of the universal radial distribution of satellite galaxies found in cosmological dark matter halos (Gill et al. 2004a, 2004b). Even though satellite–satellite interactions are unimportant for the majority of satellite galaxies, there exists a sub-population for which this needs to be investigated in more detail and more carefully, respectively.

We also noted that there is a degeneracy between the influence of the host halo and the interactions with the companion satellites which can only be disentangled with an appropriate resolution for both the actual N-body simulation and the halo finding technique. We therefore applied a new method for identifying gravitationally bound objects in cosmological N-body simulations. This new technique is based upon the adaptive grid structures of the open source adaptive mesh refinement code `MLAPM` (Knebe, Green, & Binney 2001). The halo finder is called `MHF` and acts on the same accuracy level as the actual simulation. A more thorough study of the functionality of `MHF` is presented in Gill, Knebe, & Gibson (2004a). A detailed analysis of the degeneracy between influence of the host halo and interactions with companion satellites can be found in a companion paper, too (Gill, Knebe, & Gibson 2004b).

Acknowledgments

The simulations presented in this paper were carried out on the Beowulf cluster at the Centre for Astrophysics & Supercomputing, Swinburne University, Melbourne.

References

Barnes, J. E., & Hut, P. 1986, Natur, 324, 446
Benson, A. J., Frenk, C. S., Lacey, C. G., Baugh, C. M., & Cole, S. 2002, MNRAS, 333, 177
Bertschinger, E. 1998, ARA&A, 36, 599
Davis, M., Efstathiou, G., Frenk, C. S., & White, S. D. M. 1985, ApJ, 292, 371
Efstathiou, G., Davis, M., White, S. D. M., & Frenk, C. S. 1985, ApJS, 57, 241
Gill, S. P. D., Knebe, A., & Gibson, B. K. 2004a, MNRAS, in press
Gill, S. P. D., Knebe, A., & Gibson, B. K. 2004b, in press
Gill, S. P. D., Knebe, A., Gibson, B. K., & Dopita, M. A. 2004c, MNRAS, submitted
Hayashi, E., Navarro, J., Taylor, J., Stadel, J., & Quinn, T. 2003, ApJ, 584, 541
Ibata, R. A., & Lewis, G. F. 1998, ApJ, 500, 575
Johnston, K., Hernquist, L., & Bolte, M. 1996, ApJ, 465, 278
Klypin, A. A., & Shandarin, S. F. 1983, MNRAS, 204, 891
Klypin, A., Kravtsov, A., Valenzuela, O., & Prada, F. 1999, ApJ, 522, 82
Knebe, A., Green, A., & Binney, J. 2001, MNRAS, 325, 845
Knebe, A., Kawata, D., Gill, S. P. D., & Gibson, B. K. 2004, in preparation
Moore, B. 1996, Natur, 379, 613
Spergel, D. N., Verde, L., Peiris, H. V., Komatsu, E., Nolta, M. R., Bennett, C. L., Halpern, M., Hinshaw, G., Jarosik, N., Kogut, A., Limon, M., Meyer, S. S., Page, L., Tucker, G. S., Weiland, J. L., Wollack, E., & Wright, E. L. 2003, ApJS, 148, 175
van den Bergh, S. 1994, ApJ, 428, 617
White, S. D. M., & Rees, M. 1978, MNRAS, 183, 341
Zhao, H. 1998, ApJL, 500, 149